Neuro-Oncology

Neuro-Oncology 16(4), 540–551, 2014
doi:10.1093/neuonc/not222
Advance Access date 4 December 2013

Functional role of endothelial adhesion molecules in the early stages of brain metastasis

Manuel Sarmiento Soto, Sébastien Serres, Daniel C. Anthony, and Nicola R. Sibson

CR-UK/MRC Gray Institute for Radiation Oncology and Biology, Department of Oncology, University of Oxford, Churchill Hospital, Oxford, UK (M.S.S., S. S., N.R.S.; Department of Pharmacology, University of Oxford, Oxford UK (D.C.A.)

Corresponding author: Nicola R. Sibson, PhD, Experimental Neuroimaging Group, Radiobiology Research Institute, Churchill Hospital, Oxford, OX3 7LJ, UK (nicola.sibson@oncology.ox.ac.uk).

Background. Cellular adhesion molecules (CAMs), which are normally associated with leukocyte trafficking, have also been shown to play an essential role in tumor metastasis to non-CNS sites. However, the role played by CAMs in brain metastasis is largely unexplored. It is known that leukocyte recruitment to the brain is very atypical and that mechanisms of disease in peripheral tissues cannot be extrapolated to the brain. Here, we have established the spatiotemporal expression of 12 key CAMs in the initial phases of tumor seeding in 2 different models of brain metastasis.

Methods. BALB/c or SCID mice were injected intracardially (10^5 cells/100 μL phosphate-buffered saline with either 4T1-GFP or MDA231BR-GFP cells, respectively ($n = 4–6$/group), and expression of the CAMs was determined by immunohistochemistry and immunofluorescence colocalisation.

Results. Endothelial expression of E-selectin, VCAM-1, ALCAM, ICAM-1, VLA-4, and β_4 integrin was markedly increased early in tumor seeding. At the same time, the natural ligands to these adhesion molecules were highly expressed on the metastatic tumor cells both in vitro and in vivo. Two of these ligands showed particularly high tumor cell expression (ALCAM and VLA-4), and consequently their functional role in tumor seeding was determined. Antibody neutralization of either ALCAM or VLA-4 significantly reduced tumor seeding within the brain (>60% decrease in tumor number/mm^2 brain; $P < .05–0.01$).

Conclusions. These findings suggest that ALCAM/ALCAM and VLA-4/VCAM-1 interactions play an important functional role in the early stages of metastasis seeding in the brain. Moreover, this work identifies a specific subset of ligand-receptor interactions that may yield new therapeutic and diagnostic targets for brain metastasis.

Keywords: brain, cellular adhesion molecules, endothelium, metastasis, mouse, neutralizing antibody.

Brain metastasis is estimated to occur in 10%–30% of all cancer patients and most commonly originates from one of 3 primary cancers: lung (40%–50%), breast (15%–25%), and melanoma (5%–20%).[1] Importantly, the brain is the only site of tumor relapse in ~60% of lung cancer patients, ~25% of breast cancer patients, and ~55% of melanoma patients[2] and is a frequent site of therapeutic failure. The process of brain metastasis depends on the success of several steps including cancer cell dissociation from the primary tumor, dissemination and survival within the circulation, adhesion and subsequent penetration of the blood brain barrier, and proliferation within the brain microenvironment. The initial stages of brain metastasis are difficult to detect in vivo, and this is one of the primary reasons for poor prognosis.[3]

Critically, our understanding of metastatic progression in the brain remains incomplete. The distinct steps of tumor cell extravasation and subsequent metastatic colonization are mediated by a variety of receptor-ligand pairs on opposing cell type; therefore, interactions of tumor cells with components of the brain microenvironment are crucial determinants in their progression towards metastasis, dormancy, or clearance.[4] Central to these interactions is the expression of cell adhesion molecules (CAMs), cell surface receptors, ligands, and growth factors, which can influence both progression and tumor phenotype as metastases develop.[5] At the same time, in vitro studies have indicated that functional activation of tumor cell surface markers may promote metastasis through a combination of altered adhesive and migratory cell functions.[6]

Received 12 June 2013; accepted 20 September 2013

Previous work at other metastatic sites, such as lung and liver, have suggested a role for several CAMs in tumor cell adhesion and extravasation;[4,7] however, little is known about their role in brain metastasis. The primary reason for our poor understanding of the role of CAMs in brain metastasis is the unique nature of the brain microenvironment, which means that processes in other organs cannot simply be extrapolated to the brain. For example, vessels in bone marrow and liver are fenestrated,[8] while the endothelial cells in the brain exhibit special tight junctions and are therefore largely impermeable to many molecules. Moreover, the endothelial cells are closely surrounded by a double layer of basal lamina, and astrocyte end-feet closely ensheath these layers, forming the glial limitans. This blood brain barrier confers a significant and unique challenge to extravasating metastatic cells that is not present elsewhere in the body. At the same time, it has become clear that the inflammatory response of the brain is markedly different to that of systemic organs,[9] and thus even the CAM profile of the brain endothelium cannot be considered to follow the pattern seen in liver, lung, or bone. In vitro studies of metastatic tumor cells have provided some information on tumor cell adhesion to brain endothelial cells and subsequent transendothelial migration,[10] but these are limited by their nature in vitro. At the same time, in vivo studies, although scarce, have demonstrated that metastatic extravasation into the brain takes significantly longer than it does in other organs,[11] supporting the concept that this process may require different mechanisms to those involved at other metastatic sites. Thus, the role of specific CAMs during metastatic tumor seeding to the brain remains unclear.

The primary aim of this study, therefore, was to determine the expression of 12 different CAMs/ligands in the early stages of metastasis pathogenesis in the brain in vivo during initial seeding to the brain. The 12 CAMs were chosen on the basis of previous work at other metastatic sites, and/or their involvement in other neurological diseases. Expression of the same molecules was also assessed on the metastatic tumor cells themselves both in vivo and in vitro. Subsequently, we sought to determine whether 2 of the CAMs that were found to be upregulated early on the endothelium (ALCAM and VCAM-1) were functionally involved in the initial steps of metastasis seeding to the brain.

Materials and Methods

In Vivo Models

As a primary model system, the metastatic murine mammary carcinoma 4T1-GFP cell line was used.[12] Female BALB/c mice, 7–8 weeks old, were anesthetized with 2%–3% isoflurane in oxygen and injected intracardially into the left ventricle under ultrasound guidance (VEVO 770, Visualsonics) with 1×10^5 primary 4T1-GFP cells in 100 μL phosphate-buffered saline (PBS). Those CAMs showing significant levels of expression at day 10 and colocalization with endothelial cell markers were further assessed at an earlier time point (day 5) in order to evaluate their role in the early arrest/extravasation stage of metastasis ($n = 4$ per time point).

As a second model, a subclone of a metastatic human breast carcinoma that preferentially metastasizes to the brain,[13] MDA231BR-GFP (a kind gift of Dr Patricia Steeg, National Cancer Institute, USA) was used. Female SCID mice, 7–8 weeks old, were anesthetized as above and injected intracardially with 1×10^5 MDA231BR-GFP cells in 100 μL PBS ($n = 4$). A later time point was chosen for investigation, as previous experiments have shown that this is a slower-growing tumor cell line; by day 21, the colonies were of a similar size to those seen at day 10 in the 4T1-GFP model.[14] All experiments were approved by the UK Home Office.

Immunohistochemistry

Expression was assessed for the following adhesion molecules and ligands: vascular cell adhesion molecule-1 (VCAM-1), intercellular adhesion molecule-1 (ICAM-1), activated leukocyte cellular adhesion molecule (ALCAM), E-selectin, P-selectin, L-selectin, P-selectin glycoprotein ligand-1 (PSGL-1), integrin α_4 (subunit of the integrin VLA-4), very late antigen 4 (VLA-4 or integrin $\alpha_4\beta_1$), integrin β_4, lymphocyte function-associated antigen-1 (LFA-1 or integrin $\alpha_L\beta_2$ or CD11a/CD18), and vascular apoptosis-inducing protein-1 (VAP-1).

All animals were transcardially perfusion-fixed under terminal anesthesia with 0.9% heparinized saline followed by 200 mL of periodate lysine paraformaldehyde (PLP) containing only 0.025% glutaraldehyde (PLP_{light}). The brains were postfixed, cryoprotected, embedded, and frozen in isopentane at −40°C. For immunohistochemical detection of the 12 proteins, 10 μm sections were collected onto gelatinized slides, washed in PBS (Thermo Fisher Scientific), and quenched using 1% hydrogen peroxide (Sigma Aldrich) in methanol. Slides were rewashed in PBS, placed in a Shandon Sequenza staining clip (Thermo Fisher Scientific), and washed again. Sections were blocked using 10% normal rabbit, goat or horse serum (depending on the antibody studied) (NRS/NGS/NHS; Vector Laboratories) in Dulbecco's PBS (Invitrogen). Slides were then incubated for 16 hours with the appropriate primary antibody (see Primary Antibodies section) in PBS containing 1% NRS or NGS or NHS and 0.05% Tween at 4°C. For all of the 12 CAMs analyzed, negative control experiments (no primary antibody) were included to verify specific immunostaining of CAMs; no immunoreactive staining was evident in these negative controls. After rinsing in PBS, sections were incubated for 1 hour with the appropriate secondary antibody (see Secondary Antibodies section). Slides were washed and then incubated in Vectorelite ABC kit (1:1:100; Vector Laboratories) for 45 minutes. The peroxidase was visualized using 3, 3′-diaminobenzidine (DAB; Sigma Aldrich). Sections were counterstained with cresyl violet (Sigma Aldrich). Finally, sections were mounted and coverslipped using DPX mounting solution (Thermo Fisher Scientific).

All sections were counterstained with cresyl violet, under which conditions the tumor boundary was readily delineated. To determine CAM expression levels, it was necessary to account for variations in DAB background staining (brown). To this end, multiple pictures at > x200 magnification (white balance corrected) were taken from regions outside the tumor periphery and used as reference images to establish the basal level of DAB staining within individual sections. Expression of CAMs was considered positive only where DAB immunoreactivity was above that seen in background reference images and was clearly cell-specific (Supplementary data, Table S1).

To assess areas of individual molecule expression, photomicrographs of each brain section were obtained using a Nikon E800 microscope coupled to a RoHS camera. Images were analyzed using Qcapture Pro software (Qimaging) and Adobe Photoshop CS4 (Adobe Systems Incorporated). Areas of expression, as a percentage of total tumor area, were quantified for each marker on ≥ 5 sections per animal.

Immunofluorescence

Immunofluorescent colocalization of each biomarker with endothelial cells, microglia, astrocytes, or tumor cells was determined using either fluorescent tyramide signal amplification (TSA, PerkinElmer) or secondary antibodies attached to different dyes (AMCA or Cy3). Similarly, expression of each biomarker on resting and stimulated tumor cells was evaluated using Cy3 dye.

Sections were quenched with 1% hydrogen peroxide in PBS, streptavidin- and biotin-blocked (SP-2002; Vector Laboratories) and then incubated

with Tris-NaCl blocking buffer (TNB, PerkinElmer). Sections were subsequently incubated for 16 hours at 4°C with the appropriate primary antibody (see Primary Antibodies section), rinsed with PBS, and incubated with the appropriate secondary antibody (see Secondary Antibodies section) in TNB for 30 minutes. Sections were then washed with PBS, incubated with streptavidin-HRP (1:200; PerkinElmer) in TNB for 30 minutes, washed, and incubated for 8 minutes in the dark with TSA-biotin (1:100; PerkinElmer) in amplification buffer (PerkinElmer). Slides were washed and incubated with a streptavidin-Cy3 fluorophore (1:200; Invitrogen) for 30 minutes. To detect the other fluorophore, the AMCA-conjugated secondary antibody was added at the same time as streptavidin-Cy3. Slides were coverslipped using Vectashield mounting medium (Vector Laboratories).

Images were acquired using an inverted confocal microscope (LSM-710; Carl Zeiss Microimaging) or Leica DM IRBE (Leica) attached to a camera (Hamamatsu, Japan), and analyzed using either Zen (Carl Zeiss) software or Simple PCI (Hamamatsu) software, respectively. Detection ranges were set to eliminate crosstalk between fluorophores: 409–485 nm for AMCA, 494–553 nm for GFP, and 564–712 nm for Cy3.

In Vitro Study

CAM expression was also analyzed on both cell lines (4T1-GFP and MDA231BR-GFP) in vitro. Cells were seeded onto 96-well plates and cultured for 48 hours in Dulbecco's Modified Eagle's Medium (DMEM) medium (10% fetal bovine serum, 1% glutamine). For the stimulated conditions, 4T1-GFP cells were incubated with either 55% mouse (BALB/c) plasma in DMEM or 50 ng/mL mouse CXCL12 (SDF1α; PeproTech). MDA231BR-GFP cells were incubated with 55% human plasma in DMEM or 50 ng/mL human CXCL12 (SDF1α (PeproTech). Cells were exposed to the stimulus for 6 hours. CXCL12 was chosen because its receptor, CXCR4, is present in both cell lines and is highly activated on several metastatic tumor cells that actively metastasize to the brain.[5,15]

Following exposure to the different stimuli, cells were washed 3 times with PBS and fixed for 10 minutes with 4% PFA. Subsequently, cells were washed with PBS/Tween for 10 minutes, and then endogenous biotin and streptavidin were blocked, respectively. Cells were then incubated with TNB blocking serum (PerkinElmer) for 1 hour and then with the appropriate primary antibodies (see Primary Antibodies section) overnight at 4°C. Cells were washed, incubated with the appropriate secondary biotinylated antibody (see Secondary Antibodies section) for 1 hour and then washed and incubated for 30 minutes with streptavidin-Cy3 fluorophore. Finally, cells were washed in mounting medium with DAPI to stain nuclei. Cell immunofluorescence was analyzed using and IN Cell Analyzer 1000 (GE healthcare). The 96-well plate was positioned on the stage, and a 20x lens was used to acquire immunofluorescent images of 200 cells per well using 3 different filters: DAPI 360 nm excitation and 480 nm emission; GFP 480 nm and 510 nm, respectively; and Cy3 580 nm and 640 nm, respectively.

Primary Antibodies

The following primary antibodies were used for adhesion molecule or ligand detection: anti-L-selectin antibody (1:50; Santa Cruz Biotechnology); anti-VCAM-1 antibody (1:250; Millipore); anti-integrin α_4 (1:250; Santa Cruz Biotechnology); anti-ALCAM antibody (1:1000; R&D Systems); anti-ICAM-1 antibody (1:1000; R&D Systems); anti-E-selectin antibody (1:50; R&D Systems); anti-P-selectin antibody (1:50; BD Biosciences); anti-VLA-4 antibody (1:100; Abcam); anti-integrin β_4 (1:300; Santa Cruz Biotechnology); anti-PSGL-1 (1:100; Santa Cruz Biotechnology); anti-LFA-1 antibody (1:200; Abcam), and anti-VAP1 antibody (1:100; Abcam). For colocalization studies, anti-GFAP antibody (1:400; Dako) was used for astrocyte detection, anti-Iba-1 (1:400; Wako Chemicals) was used for microglial detection, and anti-vWF (1:200; Millipore) antibodies were used to identify endothelial cells. Tumor cells were detected by virtue of their GFP tag.

Secondary Antibodies

The following secondary antibodies were used as appropriate: Cy3-streptavidin conjugate (1:200;Invitrogen); anti-rabbit AMCA-conjugated (1:100; Vector Laboratories); biotinylated polyclonal antibody to chicken raised in rabbit (Abcam); biotinylated polyclonal antibody to goat raised in horse (Vector Laboratories); polyclonal antibody to rat raised in rabbit (Vector Laboratories); and biotinylated polyclonal to rabbit raised in goat (Vector Laboratories).

Neutralizing Antibody Study

To block specific tumor-expressed ligands, MDA231BR-GFP cells were incubated with different concentrations (50 or 100 μg/mL) of anti-ALCAM or anti-α_4 antibodies for either 1 or 2 hours to determine maximum neutralization efficiency. In the case of VLA-4 neutralization, owing to the heterodimeric structure (composed of integrins α_4 and β_1), blockade of the α_4 chain provided selective inhibition of the whole protein. In order to ascertain optimal blocking efficiency, ALCAM and VLA-4 expression was quantified via immunofluorescence in at least 300 cells per treatment group.

For subsequent in vivo experiments, MDA231BR-GFP cells were incubated for 2 hours with either anti-ALCAM or anti-α_4 neutralising antibodies at 100 μg/mL (R&D system), based on the results of the dose-response experiments, prior to intracardiac injection in female SCID mice as above ($n = 5$/group). In addition, a mouse IgG1 isotype control antibody was used to assess the effect of a non-anti-CAM antibody on metastatic burden. To this end, a third set of MDA231BR-GFP cells was incubated with this isotype-control (Cell Signaling Technology). under the same conditions as the neutralizing antibodies. and subsequently injected intracardially into SCID mice as above ($n = 5$). Brains were collected at day 21, and the number of metastatic colonies was counted. Female SCID mice ($n = 5$) injected with naive MDA231BR-GFP cells (1×10^5cells/100 μL PBS) were used as the control group.

Assessment of Metastasis Morphology Following CAM Blockade

In general, 3 different tumor colony morphologies were found in animals injected with either naive MDA231BR-GFP cells or incubated with neutralizing antibody prior to intracardiac injection: (i) primarily perivascular, co-optive growth along local vessels; (ii) small perivascular colonies with minimal co-optive growth; and (iii) larger colonies showing parenchymal invasion with or without co-optive growth (See Fig. 5). With regards to the co-optive growth pattern, the degree of co-option was quantified as the number of vessels that were encompassed (co-opted) by a single tumor. In each case, the percentage of all tumors falling within each morphological category was calculated.

Cell Viability Assay

To assess the effect of CAM neutralization on MDA231BR-GFP cells, proliferation and viability were measured using an MTT (3-[4,5-dimethylthiazol-2-yl]-2,5 diphenyl tetrazolium bromide) assay. Cells were coated onto a 96-well plate and incubated with SCID mouse plasma for either 6 or 24 hours prior to and after incubation with neutralizing antibodies (50 and 100 μg/mL). After that, 50 μL of 5 mg/mL MTT was added to each well, and the plates were incubated for 4 hours at 37 °C in 5% CO_2. Media were then removed and replaced with 75 μL dimethyl sulfoxide to dissolve insoluble purple formazan dye crystals. Absorbance was measured by a photometric microplate reader (Tecan) at 570 nm within 30 minutes.

Statistics

Statistical analysis was performed using Prism (GraphPad Software Inc.). For the IHC quantitation, analysis of variance (ANOVA) was used to identify overall significant differences between the different time points, followed by pairwise unpaired *t* tests with Welch's correction for unequal variances to identify specific differences between the groups. To analyze differences between groups treated with different concentrations of neutralizing antibodies and control groups, average number of colonies, volume, and number of vessels co-opted by individual tumors were compared by ANOVA followed by post hoc Dunnett's *t* tests. All data are expressed as mean ± standard error of the mean (SEM).

Results

A well-established metastatic model, induced via the hematogenous route, was employed to allow evaluation of the seeding stage of brain metastasis. Two different mammary carcinoma cell lines were used (the mouse 4T1-GFP line and the less-aggressive human MDA231BR-GFP line) to assess conservation of adhesion molecule expression. No clinical signs were evident in any of the groups.

CAM Expression in Brain Metastasis Models

Expression of the 12 different CAMs/ligands was first quantified as a percentage of the tumor area. For this purpose, tumor area was defined as not only the area covered by tumor cells but also by the glial, endothelial, or different immune cells contained within the clearly circumscribed tumor border. This is because the nature of metastatic colonies was heterogeneous and included several specific host cell populations.

ALCAM, ICAM-1 and VCAM-1 all showed upregulation in both models, with ALCAM showing the highest level of expression (~97% and ~88% tumor area; Fig. 1) and VCAM-1 the lowest (15%–20% tumor area; Fig. 1). VLA-4 (and subunit α_4) and LFA-1, cognate ligands to VCAM-1 and ICAM-1, respectively, also showed widespread expression throughout the tumor area in both models (Fig. 1). The integrin β_4 and the cell surface enzyme VAP-1, both previously implicated in metastasis, were also evaluated; integrin β_4 showed extensive expression throughout the tumor area (>80% tumor area; Fig. 1) in both models, while VAP-1 showed minimal levels of expression (Fig. 1).

Of the 3 selectins, E-selectin showed the greatest spatial extent of expression in the 4T1-GFP model (~82% tumor area; Fig. 1B), while L- and P-selectin expression were much more restricted (~8% and ~6% tumor area, respectively). In the less aggressive MDA231BR-GFP model, all 3 selectins showed similar and relatively low levels of expression (maximum ~20% tumor area). PSGL-1, a primary ligand for all 3 selectins, showed only moderate expression in both models (~16% tumor area; Fig. 1B).

Little or no constitutive expression of any of the 12 CAMs studied was found in normal naive brain (Supplementary data, Fig. S1, S2) or in metastasis-bearing brains at sites distant to metastatic foci. However, it should be noted that pan-striatal DAB staining is evident when using the anti-ALCAM antibody in both naive and metastasis-bearing brain, which is weaker and independent of the dense cell-specific staining observed at tumor sites.

Endothelial Colocalization of CAMs within the Brain Vasculature

To identify CAMs that could play a role specifically in tumor cell arrest and extravasation, their colocalization with the endothelial marker,von Willebrand Factor (vWF) was assessed. VCAM, ALCAM, and ICAM-1 all showed colocalization with the vascular endothelium, as did VLA-4 (Fig. 2). In contrast, LFA-1, the ligand to ICAM-1, was not found on the endothelial layer. Although expression of the integrin β_4 was found to colocalize with the endothelium, this tended not to be at points of contact between the metastatic colonies and brain vessels. Similarly, VAP-1 also colocalized with the endothelium, but did so predominantly on vessels surrounding the tumor colonies. All 3 selectins showed clear colocalization with tumor vessel endothelial cells (see Table 1, Fig. 2), while their ligand, PSGL-1, did not (Fig. 2). Variable expression of all 12 adhesion molecules was also evident on either astrocytes or microglia, or both (Supplementary data, Figs. S3 and S4).

Expression of the 6 CAMs showing significant levels of expression at day 10 and colocalization with endothelial cell markers was further assessed at day 5 after intracardiac injection of 4T1-GFP cells. VCAM-1 expression was notably higher at day 5 than day 10 ($P < .005$; Fig. 1B), while ICAM-1 expression was comparable at both time points (Fig. 1B). E-selectin, VLA-4, β_4, and ALCAM showed slight but significant ($P < .005$) lower levels of expression at day 5 than day 10, although expression was still marked (Fig. 1B).

Expression of CAMs on Tumor Cells

Having established the endothelial profile of CAM expression, we subsequently determined their expression on the tumor cells themselves, both in vitro and in vivo. All of the CAMs and their ligands, except L-selectin, P-selectin, and VAP-1, were expressed on the tumor cells both in vitro under all conditions and in vivo (Table 1; Fig. 3, Supplementary data, S5 and S6). The CAMs showing the highest levels of expression in the in vitro study were ALCAM, VLA-4, α_4 (subunit of VLA-4), β_4, and E-selectin, and these molecules were highly activated under any of the in vitro conditions (Figs. 3, Supplementary data, S5 and S6). Similarly, all of these molecules showed clear expression on tumor cells in vivo.

Antibody Treatment Optimization

From the above experiments, we identified 2 CAMs (ALCAM and VCAM-1) that are strongly upregulated early in metastasis development on the endothelium and 2 CAMs (ALCAM and VLA-4) for which the natural ligands are also strongly expressed on the metastatic tumor cells. These findings led us to hypothesize that ALCAM/ALCAM and VCAM-1/VLA-4 interactions may play a functional role in the initial steps of metastasis seeding to the brain. To test this hypothesis, either ALCAM or VLA-4 ($\alpha_4\beta_1$) on the surface of MDA231BR-GFP cells was blocked by incubation with neutralizing antibodies to prevent binding to their target adhesion molecules on the vascular endothelium. Owing to a lack of specific VLA-4 neutralizing antibody, an anti-α_4 antibody was used, based on our observations that α_4 expression did not exceed that of VLA-4, and was thus unlikely to reflect expression of other integrins containing this subunit.

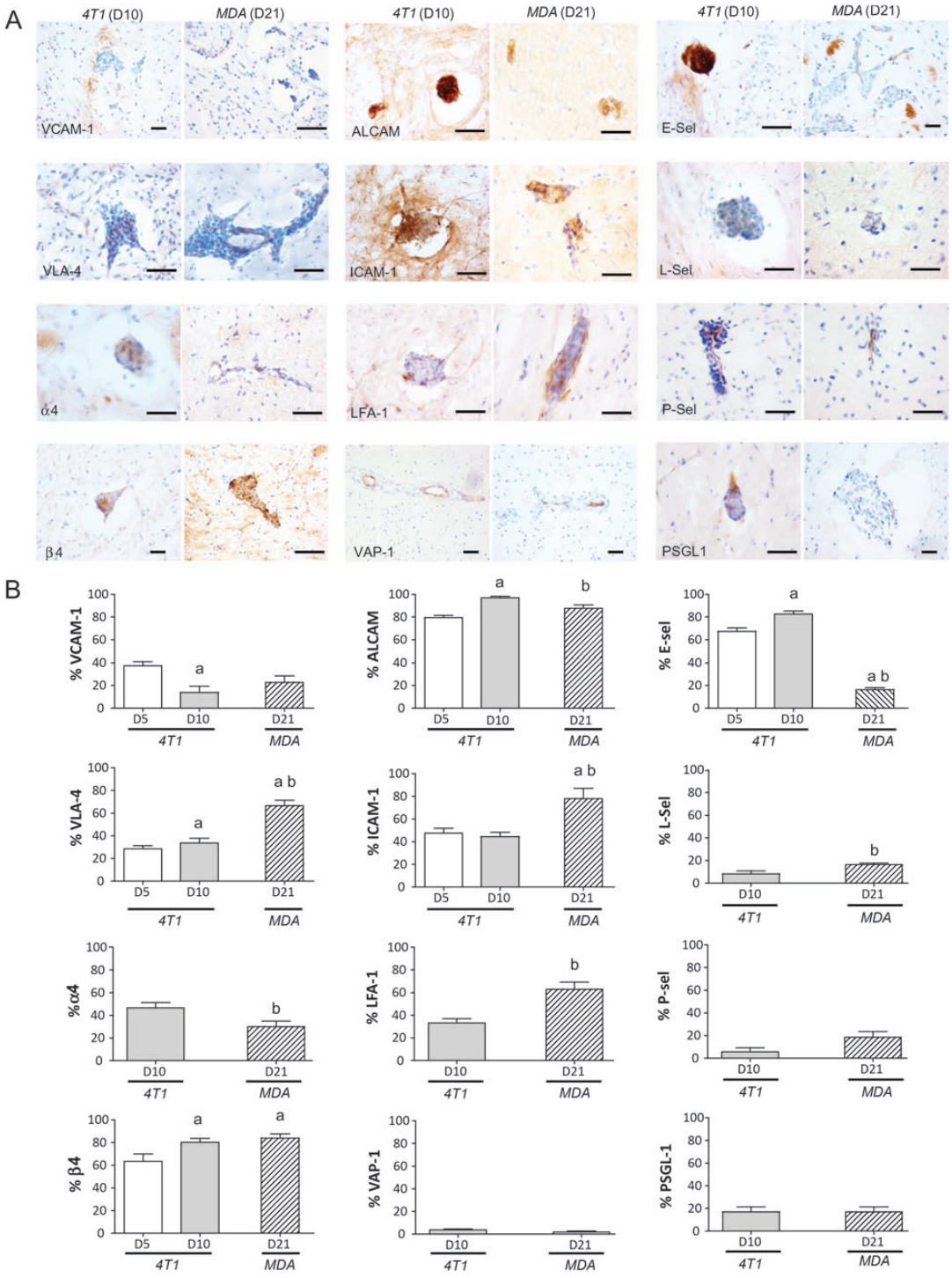

Fig. 1. Expression of cellular adhesion molecules. (A) Immunohistochemical detection of cell adhesion molecules at metastatic foci in BALB/c (4T1(D10)) and SCID (MDA(D21)) mice injected intracardially with 1×10^5 4T1-GFP or MDA231BR-GFP cells, respectively, in 100μl PBS. Images are shown for day 10 in the 4T1-GFP model and day 21 in the MDA231BR-GFP model. Scale bar 50 μm. (B) Graphs showing quantitative analysis of the expression of cell adhesion molecules within the tumor area in BALB/c (days 5 and 10) and SCID mice (day 21) injected intracardially with 1×10^5 4T1-GFP (4T1) or MDA231BR-GFP cells (MDA), respectively, in 100 μL PBS. Results are expressed as the percentage area of biomarker expression compared with the total tumor area for each time point. Statistical significances are compared with the 4T1-GFP model day 5(a) and day 10(b); ($P < .05–0.001$. $n = 4$/time point).

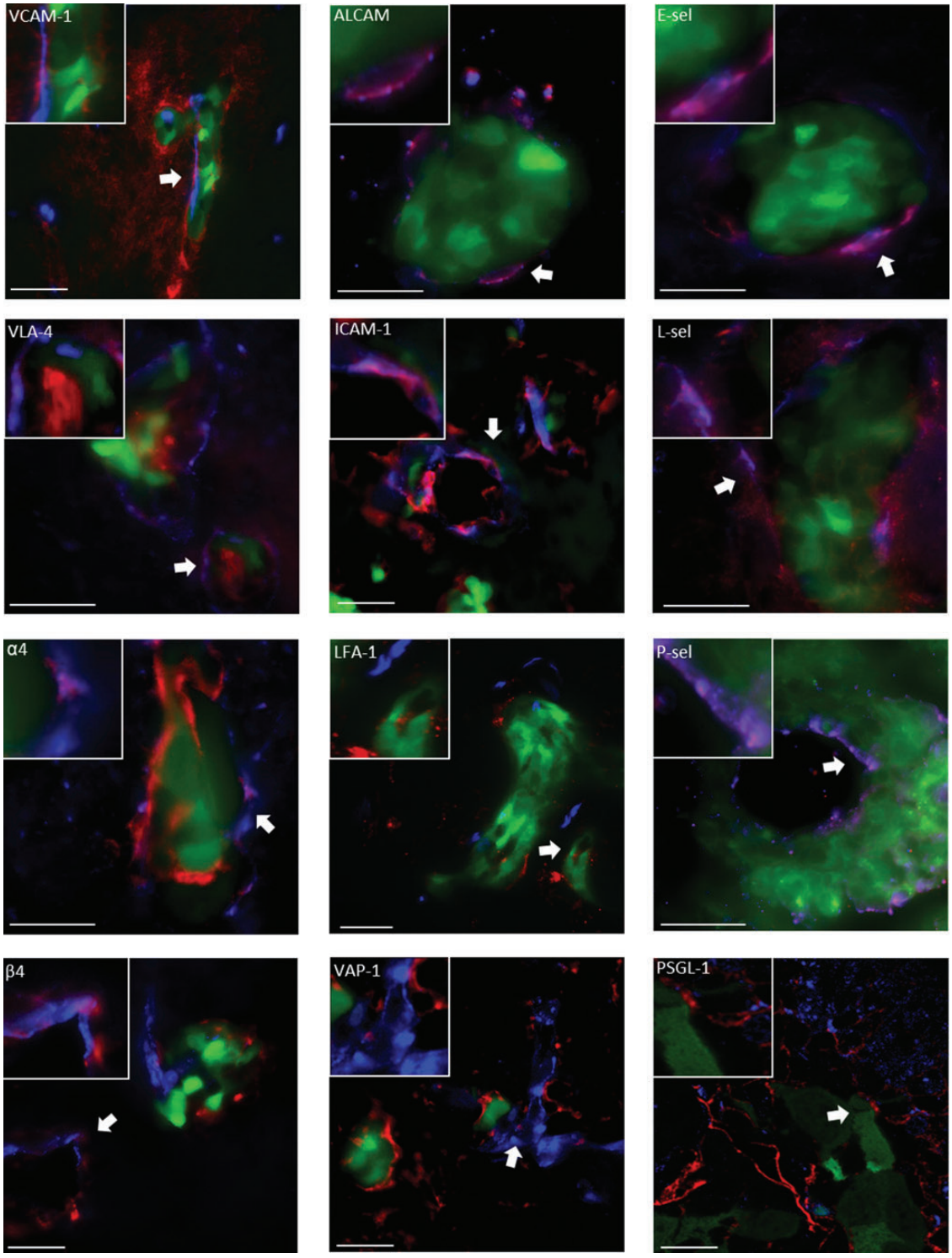

Fig. 2. Colocalization of adhesion molecules with endothelial cells. Triple-color fluorescence images showing colocalization (arrows) between tumor cells and endothelial marker von Willebrand Factor (vWF) in the 4T1-GFP model. All tumor cells injected were GFP positive, and therefore the green fluorescence corresponds to tumor cells. An AMCA fluorophore was used to localize the endothelial markers, and hence the blue color reflects vWF. To detect the 12 cellular adhesion molecules, a Cy3 fluorophore was used (red). Scale bar 50 μm. High magnification insets show regions of colocalization (indicated by arrows).

Table 1. Summary of biomarker colocalization with endothelial cells, astrocytes, microglia, and tumor cells in the 4T1-GFP model

	% Expression	Endothelium	Astrocytes	Microglia	Tumor Cells			
					In vivo	In vitro	+ *plasma*	+*CXCL12*
VCAM-1	13.7 ± 15.8	+	+	+	+	+	+	+
VLA-4	33.5 ± 9.7	+	+/−	+	+	++	++	++
$\alpha 4$	46.6 ± 9.4	+	+	+	+	++	++	++
$\beta 4$	80.3 ± 7.5	+	+/−	+/−	+	++	++	++
ALCAM	97. 1 ± 3.6	+	−	+	+	++	++	++
ICAM-1	44.5 ± 7.7	+	+	+	+	+	+	+
LFA-1	33.2 ± 10.4	−	+	+	+	+	+	++
VAP-1	3.8 ± 1.5	+	+	+	−	−	−	−
E-selectin	82.7 ± 5.7	+	+	+	+	++	++	++
L-selectin	8.2 ± 6.6	+	+	+	−	−	+	−
P-selectin	5. 7 ± 7.6	+	+	+	−	−	−	−
PSGL-1	16.8 ± 13.2	−	+	+	+	+	++	+

The first column shows the highest level of expression (mean ± SEM) for each adhesion molecule. The remaining columns indicate colocalization of each adhesion molecule with endothelium (vWF), astrocytes (GFAP), microglia (Iba-1), and tumor cells (GFP). Some of the markers appeared closely associated with cellular markers, but it was not possible to determine whether they colocalized or were on a separate but closely apposed cell; in those cases +/− is used. For the in vitro study, - denotes negative expression; + 10%–50% cells positive; ++ >50% cells positive.

In the first instance, efficiency of CAM neutralization on MDA231BR-GFP cells was measured by immunofluorescence and found to be significantly reduced in both anti-ALCAM and anti-α_4 treated cells at 50 and 100 μg/mL antibody concentrations ($P <$ .0001; Fig. 4A and B, Supplementary data, S7). However, following incubation with 50 μg/mL of anti-ALCAM antibody, subsequent incubation in mouse plasma for 6 hours increased the levels of ALCAM immunofluorescence, indicating increased CAM expression on exposure to plasma. In contrast, following incubation with 100 μg/mL antibodies, no change in the level of neutralization was observed on subsequent incubation with plasma up to 24 hours for either adhesion molecule (Supplementary data, Fig. S7).

Viability and proliferation of MDA231BR-GFP cells treated with neutralizing antibodies, as determined by MTT assay, was not significantly different from that of untreated cells, either before or after incubation with plasma (Fig. 4C and D). Interestingly, however, control untreated cells incubated with plasma for either 6 or 24 hours showed a significant increase in cell viability, which was blocked by preincubation with neutralizing antibodies (Fig. 4C and D).

Metastatic Burden after Antibody-neutralization of Tumor Cells

Once the most efficient dosing regime for antibody neutralization had been established, their role in vivo was determined. Thus, SCID mice injected intracardially with either anti-α_4 or anti-ALCAM antibody-treated MDA231BR-GFP cells showed a significant reduction in the number of tumor colonies in the brain at day 21 (∼63% and ∼68%, respectively; $P < .05$; Fig. 5A). The total volume of tumor burden was also significantly reduced in the anti-ALCAM-treated group (∼73% reduction; Fig. 5A). Although a modest reduction in total tumor volume was apparent in the VLA-4 blocked group (∼25%; Fig. 5A), this was not significant compared with controls. While the control group exhibited a predominantly spherical colony phenotype (∼70% colonies; Fig. 5B and C), assessment of tumor colony shape and degree of either intravascular or perivascular co-optive growth indicated that the anti-ALCAM and anti-α_4-treated animals showed more marked vessel co-option and had the appearance of earlier stage colonies than the control group, with some appearing to still be intravascular (Fig. 5B and C). No significant differences were found between the control group and animals injected with isotype-treated cells (Fig. 5A) for any of the analyses.

Discussion

It is clear that communication between tumor cells and their host environment is essential for both initiation and progression of metastatic colonization in the brain. Yet our understanding of these tumor-host interactions is far from complete. In particular, our knowledge of the role of adhesion molecules in tumor cell arrest and extravasation is poor, and the atypical inflammatory response of the brain makes it difficult to extrapolate from other metastatic sites in the body. Here we have demonstrated, using in vivo models, that a subset of adhesion molecules (E-selectin, VCAM-1, ALCAM, ICAM-1, VLA-4, and α_4) are upregulated on the cerebral endothelium soon after metastatic cell injection into the circulation. At the same time, the natural ligands to these molecules (PSGL-1, VLA-4, ALCAM, LFA-1, and VCAM-1) are highly expressed on the tumor cells themselves. Furthermore, we have demonstrated that blocking 2 of the most strongly upregulated CAMs on the tumor cells (ALCAM and VLA-4) significantly decreased the number of metastatic colonies forming within the brain. Taken together, these findings suggest a key role for this subset of adhesion molecules in the early stages of tumor cell arrest and/or extravasation.

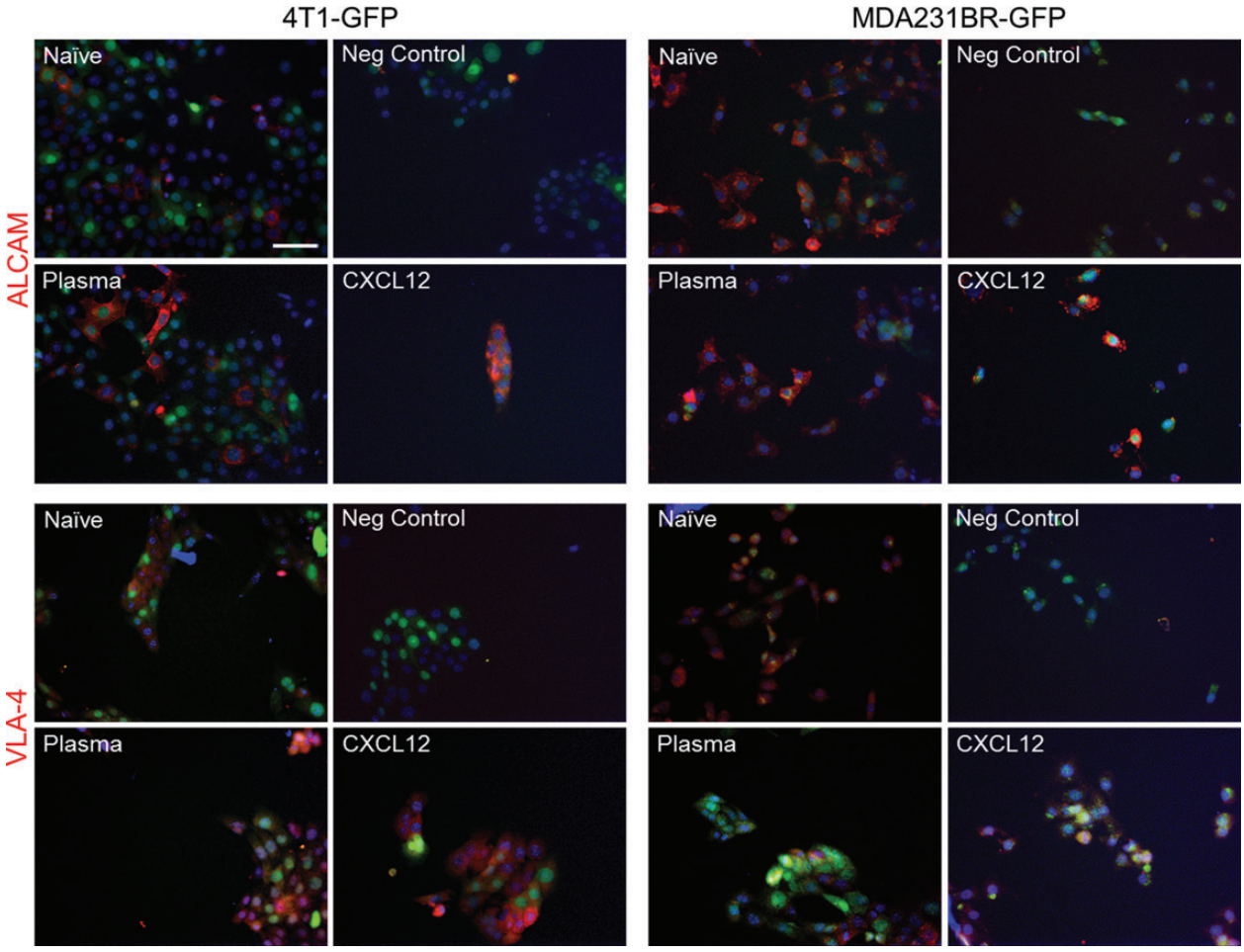

Fig. 3. In vitro expression of cellular adhesion molecules on metastatic tumor cells. Negative controls are shown for unbiased comparison with the plasma-treated, cytokine-treated, and naive groups for 2 of the most highly expressed adhesion molecules, ALCAM and VLA-4. Cells were coated onto 96-well plates and after 48 hours of growth were incubated for 6 hours with 200 μL of plasma (55%) in DMEM. Red fluorophore (Cy3) for each marker. Scale bar 100 μm. (Data for tumor cell expression of the other 10 CAMs are shown in Supplementary data, Figs. S5 and S6).

Functional Role of VLA-4/VCAM-1 in Brain Metastasis

Previous studies in other tissue beds suggest that tumor cells undergo the same succession of steps as extravasating leukocytes (ie, rolling, adhesion, and transmigration [diapedesis]), and utilize similar cell adhesion molecules.[16] Integrins are a key family of transmembrane adhesion receptors that are composed of non-covalently linked α and β subunits and have been shown to be involved in adhesion of leukocytes to the vascular endothelium.[16] Similarly, the high affinity interactions between VLA-4 ($\alpha_4\beta_1$) and VCAM-1 have been shown to promote transmigration of metastatic melanoma cells across activated human endothelial layers in vitro[17] and differential expression of VLA-4 found on metastatic versus nonmetastatic tumor cell lines. These data have been taken to suggest that VLA-4 is important in metastatic progression to the liver and lungs.[18]

To date, however, little was known of VLA-4 involvement in metastasis seeding to the brain, although blockade of VCAM-1 on cultured brain endothelial cells has been shown to reduce adhesion of metastatic Lewis lung carcinoma cells.[19] In the current study, each of our cell lines showed marked expression of both VLA-4 and α4 (subcomponent of VLA-4) both in vitro and in vivo. Moreover VCAM-1, the receptor for VLA-4, was widely expressed on the endothelium from as early as day 5 after intracardiac induction, as we have previously demonstrated. Moreover, our in vivo findings demonstrated a significant reduction in metastasis seeding to the brain following α_4 blockade on MDA231BR-GFP cells. These findings support the concept that VLA-4/VCAM-1 interactions are involved in tumor cell arrest and subsequent extravasation across the brain endothelium.

Functional Role of ALCAM in Brain Metastasis

ALCAM is a transmembrane glycoprotein that is upregulated on activated T cells and monocytes and mediates both heterophilic ALCAM-CD6 and homophilic ALCAM-ALCAM interactions. Recent work has also shown upregulation of ALCAM on endothelial cells in response to inflammatory stimuli, albeit primarily in vitro.[20,21] In the current study, ALCAM was highly expressed on tumor cells, both in vitro and in vivo, and also on tumor-associated endothelium. In contrast, expression of VAP-1, another transmembrane

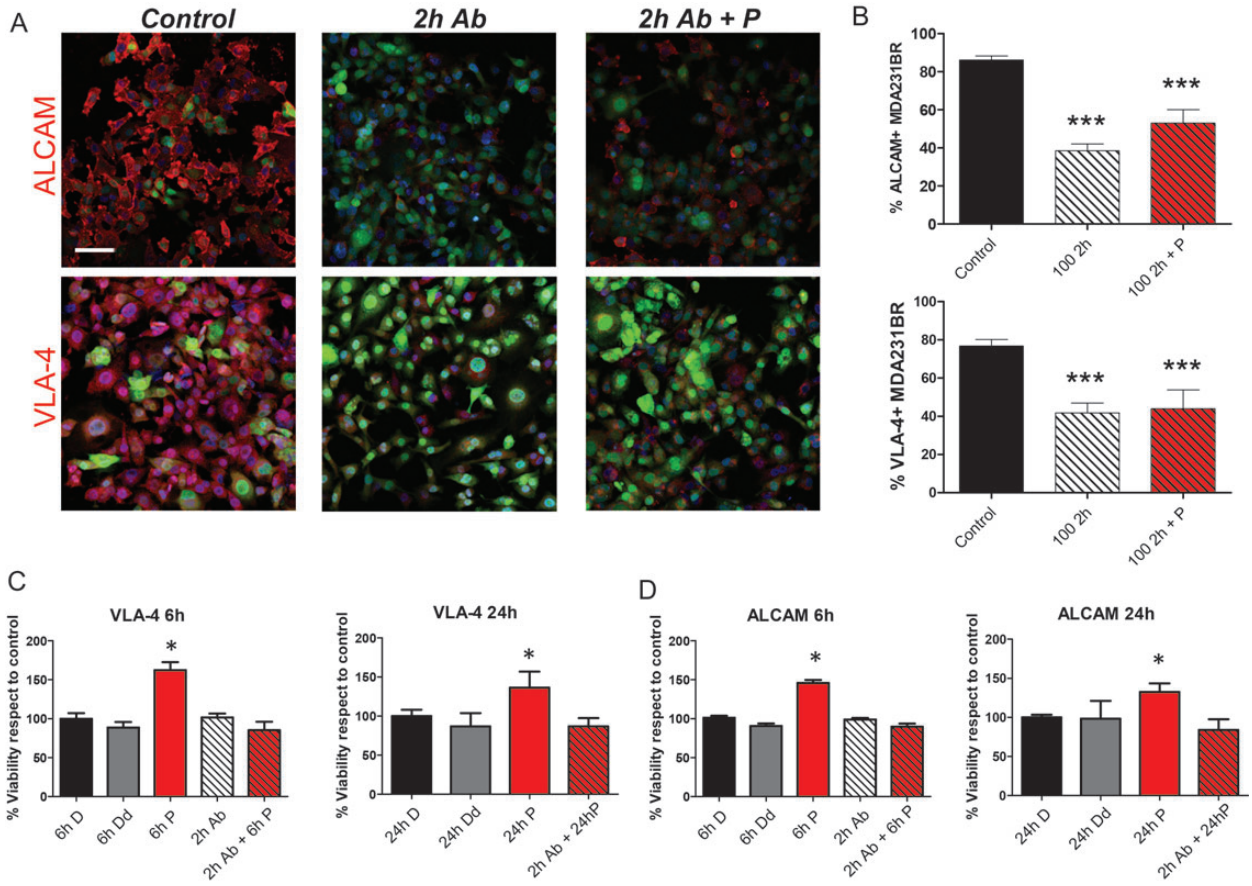

Fig. 4. Optimization of antibody blockade. (A) Confocal images of the expression of ALCAM and VLA-4 on MDA231BR-GFP cells under control conditions after 2 hours antibody incubation (100 μg/mL) with the corresponding neutralizing antibody and after the addition of plasma. Red dye (Cy3) for each marker. Scale bar 100 μm. (B) Percentage of cells showing positive ALCAM and VLA-4 expression under 3 different conditions. Statistical significances were compared with control groups ($P < .0001$). (C) MTT assay showing the viability of the cells under normal medium (100% DMEM) conditions (6hD or 24hD), 55% DMEM (6 h Dd or 24 h Dd 6-hour or 24-hour exposure to plasma (6hP or 24hP), 2 hours of incubation with the anti-α4 (VLA-4, 2 h Ab) followed by 6-hour or 24-hour exposure to mouse plasma (2hAb + 6hP or 24hP). D. As for C, but with anti-ALCAM neutralizing antibody. Percentages are expressed with respect to normal medium conditions groups. Statistical significances are compared with control 6h-24hD ($P < .05$).

glycoprotein that supports rolling, firm adhesion, and transmigration of leukocytes, was for the most part negligible on both endothelium and tumor cells. Notably, following ALCAM blockade on MDA231BR-GFP cells, a reduced number of tumor colonies were found within the brain parenchyma, and a change in metastasis morphology was apparent with a substantial proportion of colonies appearing to remain intra- or perivascular. Our results suggest both a reduction in the adherence of tumor cells to the endothelium and a slowing of the extravasation process following ALCAM blockade. These in vivo findings concur with very recent work suggesting that ALCAM may play a role in both breast cancer metastasis[22,23] and melanoma metastasis to the lung.[24] It has also been suggested that ALCAM expression on metastatic tumor cells may facilitate aggregation and binding to circulating monocytes through ALCAM-CD6 interactions, which enables the metastatic cells to circumvent immune surveillance and aids their extravasation across the endothelium.[25] Thus, neutralization of ALCAM prior to introduction into the bloodstream may reduce aggregation and binding to activated leukocytes, both enhancing immune clearance and inhibiting extravasation across the endothelium. Taken together, the above findings strongly suggest that ALCAM plays an important functional role in early tumor cell adhesion in brain metastasis.

Potential Role for ICAM-1 and E-selectin in Metastasis Seeding

Owing to its presence on many cancer cell types[26] and its potential role in metastasis,[27] it has been suggested that ICAM-1 expression may serve as a useful biomarker for tumor prognosis and progression. Marked upregulation of ICAM-1 was evident on the vascular endothelium in both models studied here and showed extensive expression extending beyond tumor margins at later time points. At the same time, expression of its cognate ligand LFA-1 was notably absent from the endothelium but highly upregulated on tumor cells both in vitro and in vivo. Upregulation of ICAM-1 was evident from as early as day 5 in the 4T1-GFP model; although LFA-1 expression on tumor cells was not as marked as VLA-4 and ALCAM, the contribution of LFA-1/ICAM-1 to tumor cell adhesion/extravasation is a focus for subsequent investigation.

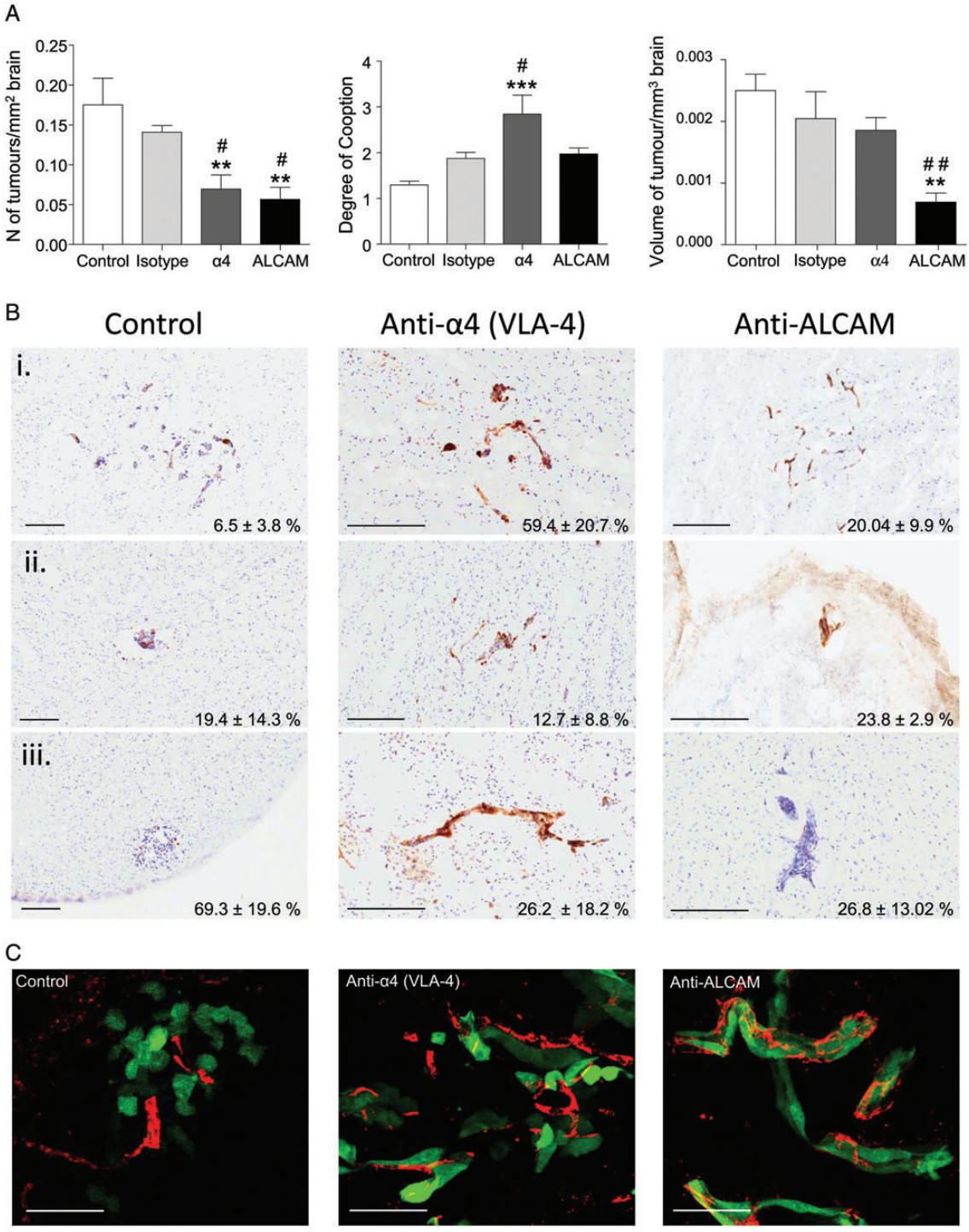

Fig. 5. Metastatic burden after intracardiac injection of antibody-blocked MDA231BR-GFP cells. (A) Graphs showing number of metastatic colonies and tumor volume per mm^3 of brain tissue after antibody treatment of MDA231BR-GFP cells (100 μg/mL anti-α_4 or anti-ALCAM or isotype IgG control) compared with untreated tumor cells ($n = 5$/group). Tumors were also assessed according to the degree of co-option (number of vessels conforming a single colony). * Denotes statistical significance versus control group (* $P < .05$, ** $P < .01$, *** $P < .001$). # Denotes statistical significance versus isotype control group (# $P < .05$, ## $P < .01$). α_4 and ALCAM groups were also significantly different in the degree of co-option and the volume of tumor burden. (B) Images illustrating the 3 main morphological phenotypes of tumor colonies observed within the brain and the percentage of all tumors in each group exhibiting each type of growth. (C) Confocal images illustrating the more perivascular/co-optive growth in the antibody-blocked groups (anti-α_4 and anti-ALCAM) compared with animals injected with the non-treated MDA231BR-GFP cells (Control). Scale bars 150 μm.

Studies in other organs such as lung and liver have demonstrated that interactions between selectins and their ligands mediate tethering and rolling of tumor cells along the vascular endothelium,[28,29] and the degree of selectin ligand expression on cancer cells correlates closely with metastatic progression.[30] Expression of all 3 selectins was evident on endothelial cells in the current study but with differential temporal and spatial expression profiles. Notably, expression of E-selectin was one of the highest measured in our brain metastatic model. However, several functional ligands exist for this glycoprotein (PSGL-1, ESL-1, and CD44[30]), and consequently blockade of ligands to E-selectin on tumor cells is not straightforward. Nevertheless, the role of E-selectin in metastasis seeding to the brain will be an important target for future studies.

In conclusion, we have determined the temporal, spatial, and cellular expression profiles of a spectrum of CAMs during the early stages of metastasis seeding in the brain. Unlike previous studies in which only single molecules or small groups of molecules have been studied, here a broad range of molecules were considered with the view that no single adhesion molecule can be solely responsible for any of these processes. Rather, it is likely that these interactions are mediated by a number of structurally diverse cell surface receptors and their ligands/counter-receptors. Our findings suggest that certain CAM/ligand interactions are important in tumor cell adhesion and extravasation. In particular, VCAM-1/VLA-4, and ALCAM/ALCAM appear to play an important functional role in metastasis seeding, while ICAM-1/LFA-1 interactions and the role of endothelial E-selectin expression also warrant further investigation. Importantly, these early markers of metastasis seeding may yield new diagnostic targets, as demonstrated in our recent work with a VCAM-1-targeted molecular MRI contrast agent,[14] as well as new therapeutic targets for brain metastasis.

Supplementary Material

Supplementary material is available online at *Neuro-Oncology* (http://neuro-oncology.oxfordjournals.org/).

Funding

This work was funded by Cancer Research UK, grant number C5255/A12678.

Acknowledgments

The authors would like to thank Dr James Larkin, Dr Ana Gil-Bernabe, Alastair Hamilton, and Claire Bristow for technical assistance and Dr Patricia Steeg (National Cancer Institute, USA) for kindly providing the MDA231BR-GFP cell line. N.R.S. supervised all of the experiments and jointly conceived the methodology with D.C.A. and M.S.S. M.S.S. and S.S. performed the in vivo experiments and conducted the histological experiments. All authors reviewed and edited the manuscript.

Conflict of interest statement. None declared.

References

1. Ranjan T, Abrey LE. Current management of metastatic brain disease. *Neurotherapeutics*. 2009;6(3):598–603.
2. Sampson JH, Carter JH Jr., Friedman AH, Seigler HF. Demographics, prognosis, and therapy in 702 patients with brain metastases from malignant melanoma. *J. Neurosurg*. 1998;88(1):11–20.
3. Eichler AF, Loeffler JS. Multidisciplinary management of brain metastases. *Oncologist*. 2007;12(7):884–898.
4. Witz IP. The involvement of selectins and their ligands in tumor-progression. *Immunol Lett*. 2006;104(1):89–93.
5. Izraely S, Klein A, Sagi-Assif O, et al. Chemokine-chemokine receptor axes in melanoma brain metastasis. *Immunol Lett*. 2010;130(1–2):107–114.
6. Felding-Habermann B, O'Toole TE, Smith JW, et al. Integrin activation controls metastasis in human breast cancer. *Proc Natl Acad Sci U S A*. 2001;98(4):1853.
7. Kannagi R, Izawa M, Koike T, Miyazaki K, Kimura N. Carbohydrate-mediated cell adhesion in cancer metastasis and angiogenesis. *Cancer Sci*. 2004;95(5):377–384.
8. Inoue S, Osmond DG. Basement membrane of mouse bone marrow sinusoids shows distinctive structure and proteoglycan composition: a high resolution ultrastructural study. *Anat Rec*. 2001;264(3):294–304.
9. Anthony DC, Couch Y, Losey P, Evans MC. The systemic response to brain injury and disease. *Brain, Behavior, and Immunity*. 2012;26(4):534–540.
10. Lorger M, Felding-Habermann B. Capturing changes in the brain microenvironment during initial steps of breast cancer brain metastasis. *Am J Pathol*. 2010;176(6):2958–2971.
11. Lorger M, Lee H, Forsyth JS, Felding-Habermann B. Comparison of in vitro and in vivo approaches to studying brain colonization by breast cancer cells. *J Neurooncol*. 2011;104(3):689–696.
12. Aslakson CJ, Miller FR. Selective events in the metastatic process defined by analysis of the sequential dissemination of subpopulations of a mouse mammary tumor. *Cancer Res*. 1992;52(6):1399–1405.
13. Yoneda T, Williams PJ, Hiraga T, Niewolna M, Nishimura R. A bone-seeking clone exhibits different biological properties from the MDA-MB-231 parental human breast cancer cells and a brain-seeking clone in vivo and in vitro. *J Bone Miner Res*. 2001;16(8):1486–1495.
14. Serres S, Soto MS, Hamilton A, et al. Molecular MRI enables early and sensitive detection of brain metastases. *Proc Natll Acad Sci*. 2012;109(17):6674–6679.
15. Ali S, Lazennec G. Chemokines: novel targets for breast cancer metastasis. *Cancer Metastasis Rev*. 2007;26(3–4):401–420.
16. Strell C, Entschladen F. Extravasation of leukocytes in comparison to tumor cells. *Cell Commun Signal*. 2008;6:10.
17. Klemke M, Weschenfelder T, Konstandin MH, Samstag Y. High affinity interaction of integrin alpha4beta1 (VLA-4) and vascular cell adhesion molecule 1 (VCAM-1) enhances migration of human melanoma cells across activated endothelial cell layers. *J Cell Physiol*. 2007;212(2):368–374.
18. Bao L, Pigott R, Matsumura Y, Baban D, Tarin D. Correlation of VLA-4 integrin expression with metastatic potential in various human tumour cell lines. *Differentiation*. 1993;52(3):239–246.
19. Sipos E, Chen L, Andras IE, et al. Proinflammatory adhesion molecules facilitate polychlorinated biphenyl-mediated enhancement of brain metastasis formation. *Toxicol Sci*. 2012;126(2):362–371.
20. Cayrol R, Wosik K, Berard JL, et al. Activated leukocyte cell adhesion molecule promotes leukocyte trafficking into the central nervous system. *Nat Immunol*. 2008;9(2):137–145.
21. Ihnen M, Kilic E, Kohler N, et al. Protein expression analysis of ALCAM and CEACAM6 in breast cancer metastases reveals significantly increased ALCAM expression in metastases of the skin. *J Clin Pathol*. 2011;64(2):146–152.

22. Wiiger MT, Gehrken HB, Fodstad O, Maelandsmo GM, Andersson Y. A novel human recombinant single-chain antibody targeting CD166/ALCAM inhibits cancer cell invasion in vitro and in vivo tumour growth. *Cancer Immunol Immunother*. 2010;59(11):1665–1674.
23. van Kilsdonk JW, Wilting RH, Bergers M, et al. Attenuation of melanoma invasion by a secreted variant of activated leukocyte cell adhesion molecule. *Cancer Res*. 2008;68(10):3671–3679.
24. Degen W, Van Kempen L, Gijzen E, et al. MEMD, a new cell adhesion molecule in metastasizing human melanoma cell lines, is identical to ALCAM (activated leukocyte cell adhesion molecule). *Am J Pathol*. 1998;152(3):805.
25. Brooks KJ, Coleman EJ, Vitetta ES. The antitumor activity of an anti-CD54 antibody in SCID mice xenografted with human breast, prostate, non-small cell lung, and pancreatic tumor cell lines. *Int J Cancer*. 2008;123(10):2438–2445.
26. Roland CL, Harken AH, Sarr MG, Barnett CC. ICAM-1 expression determines malignant potential of cancer. *Surgery*. 2007;141(6):705–707.
27. Jantscheff P, Schlesinger M, Fritzsche J, et al. Lysophosphatidylcholine pretreatment reduces VLA-4 and P-Selectin-mediated b16.f10 melanoma cell adhesion in vitro and inhibits metastasis-like lung invasion in vivo. *Mol Cancer Ther*. 2011;10(1):186–197.
28. Brodt P, Fallavollita L, Bresalier RS, Meterissian S, Norton CR, Wolitzky BA. Liver endothelial E-selectin mediates carcinoma cell adhesion and promotes liver metastasis. *Int J Cancer*. 1997;71(4):612–619.
29. Läubli H, Borsig L. Selectins promote tumor metastasis. *Semin Cancer Biol*. 2010;20(3):169–177.
30. Dimitroff CJ, Lee JY, Rafii S, Fuhlbrigge RC, Sackstein R. CD44 is a major E-selectin ligand on human hematopoietic progenitor cells. *J Cell Biol*. 2001;153(6):1277–1286.